Electronic Supplementary Material (ESI) for Journal of Materials Chemistry C
This journal is © The Royal Society of Chemistry 2014

Supplementary Information

Strain driven structural phase transformations in dysprosium doped $BiFeO_3$ ceramics

Robert C. Lennox[1], Mark C. Price[1], William Jamieson[2], Marek Jura[2], Aziz Daoud-Aladine[2], Claire A. Murray[3], Chiu Tang[3], Donna C. Arnold[1*]

[1] *School of Physical Sciences, University of Kent, Canterbury, Kent, CT2 7NH, UK*

[2] *ISIS Facility, Rutherford Appleton Laboratory-STFC, Chilton, Didcot, Oxfordshire, OX11 0QX, UK*

[3] *Diamond Light Source, Ltd., Harwell Science and Innovation Campus, Didcot, Oxfordshire, OX11 0DE, UK*

[*] *Corresponding Author, Donna C. Arnold, e-mail: d.c.arnold@kent.ac.uk, tel: 01227 827810, fax: 01227 827558*

Rietveld refinements were performed for both powder neutron and synchrotron diffraction data for all $Bi_{1-x}Dy_xFeO_3$ ($0 \geq x \geq 0.30$) materials using the General Structure Analysis System (GSAS) suite of programs.[1, 2] Initial refinements were performed for the synchrotron diffraction data collected for the x = 0, 0.02 and 0.05 materials using the *R*3*c* model for approximately 43 variables including 18 background coefficient's fitted using a shifted Chebyschev function and peak shape fitted using a Pseudo-Voigt function. The U*iso* were fixed to 1.00 (Ui/Ue*100) and the fractional occupancies of the atoms not refined. Eight spherical Harmonic order (ODF) terms were also refined in a cylindrical geometry in order to mitigate against surface roughness effects introduced by preparation of the sample for analysis. In all cases the Texture Index was close to 1 indicating that the sample is randomly orientated. Powder neutron diffraction refinements were performed for x = 0 and 0.05 materials for approximately 37 variables including 18 back ground coefficients fitted in a shifted Chebyschev function and peak shape was fitted using a Pseudo-Voigt function for time-of-flight data. An absorption coefficient was also refined in order to model absorption effects resulting from the high neutron absorption observed for dysprosium. Refinement parameters are given in tables S1 and S2 with the refinement profiles in figures S1 and S2 for synchrotron and neutron diffraction refinements respectively.

Table S1: *Rietveld refinement parameters for the refinement of powder synchrotron diffraction data collected for $BiFeO_3$, $Bi_{0.98}Dy_{0.02}FeO_3$ and $Bi_{0.95}Dy_{0.05}FeO_3$ materials using the rhombohedral, R3c model.*

Parameter	**$BiFeO_3$**	**$Bi_{0.98}Dy_{0.02}FeO_3$**	**$Bi_{0.95}Dy_{0.05}FeO_3$**
R_{wp}	10.98	11.93	15.11
R_p	8.45	9.06	11.09
a (Å)	5.57893(3)	5.57716(9)	5.57447(5)
b (Å)	5.57893(3)	5.57716(9)	5.57447(5)
c (Å)	13.86952(7)	13.8640(2)	13.8541(2)
Cell Volume (Å)	373.847(3)	373.46(1)	372.835(7)
Bi/Dy (0,0,0)			
Bi/Dy Ui/Ue*100	1.00	1.00	1.00
Fe (0,0,*z*)	0.2206(1)	0.2219(2)	0.2222(2)
Fe Ui/Ue*100	1.00	1.00	1.00
O (*x*,*y*,*z*)	0.444(1) 0.018(2) 0.9524(6)	0.446(2) 0.022(2) 0.9535(6)	0.446(3) 0.025(3) 0.955(1)
O Ui/Ue*100	1.00	1.00	1.00
Texture Index	1.0062	1.0009	1.0070
Bi-O lengths x 3 (Å)	2.519(7)	2.510(8)	2.50(1)
Bi-O lengths x3 (Å)	2.278(7)	2.274(8)	2.28(1)
Fe-O bond lengths x 3 (Å)	2.108(9)	2.10(1)	2.07(2)
Fe-O bond lengths x 3 (Å)	1.954(8)	1.971(9)	1.99(2)
Fe-O-Fe bond angle (^{o})	154.9(4)	154.2(4)	153.9(6)

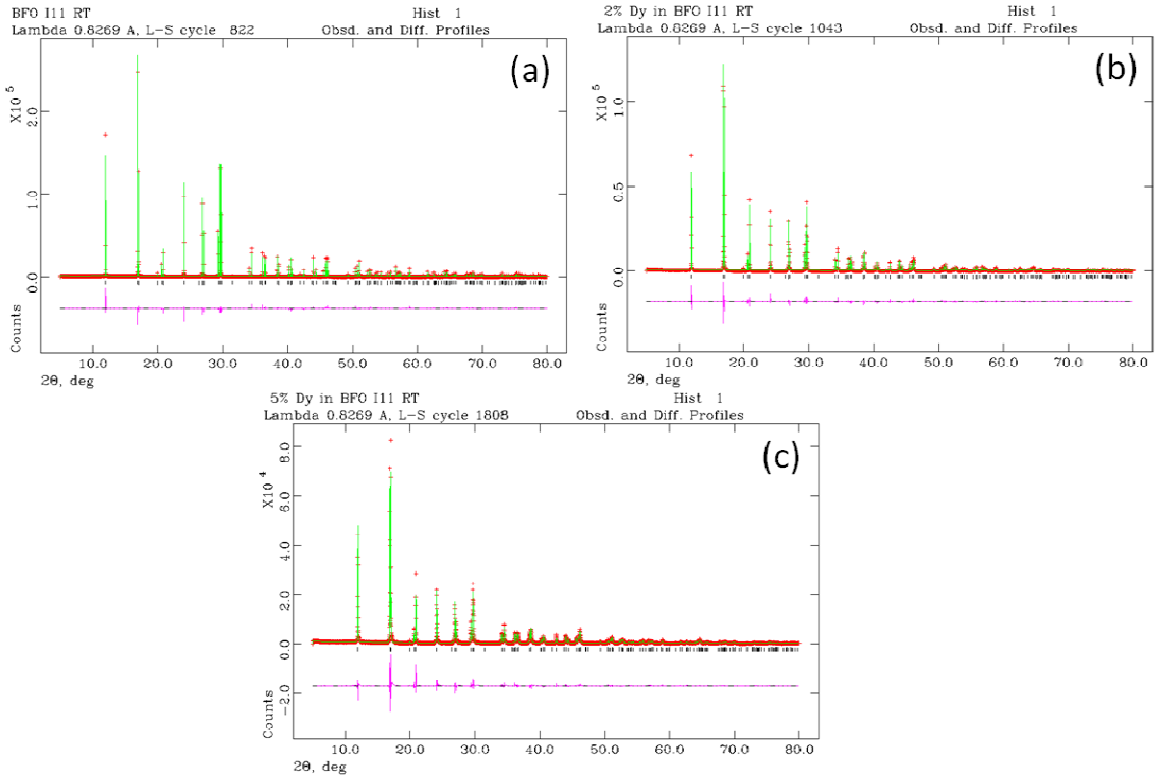

Figure S1: *Rietveld refinement profiles for data fitted using the R3c model to synchrotron diffraction data collected for (a)* $BiFeO_3$*, (b)* $Bi_{0.98}Dy_{0.02}FeO_3$ *and (c)* $Bi_{0.95}Dy_{0.05}FeO_3$*. The red circles represent the observed data, the green line represents the calculated model and the pink line represents the difference.*

Table S2: *Rietveld refinement parameters for the refinement of powder neutron diffraction data collected for $BiFeO_3$ and $Bi_{0.95}Dy_{0.05}FeO_3$ materials using the rhombohedral, R3c model.*

Parameter	$BiFeO_3$	$Bi_{0.95}Dy_{0.05}FeO_3$
Rwp	14.22	8.29
Rp	14.32	9.09
χ^2	1.543	8.891
a (Å)	5.58197(3)	5.5730(1)
b (Å)	5.58197(3)	5.5730(1)
c (Å)	13.87773(9)	13.8480(4)
Cell Volume (Å)	374.476(4)	372.48(2)
Bi/Dy (0,0,0)		
Bi/Dy Ui/Ue*100	0.34(3)	0.73(5)
Fe (0,0,*z*)	0.22109(8)	0.22159(9)
Fe Ui/Ue*100	0.16(3)	0.52(5)
O (*x*,*y*,*z*)	0.4460(2) 0.0175(3) 0.9523(1)	0.4425(3) 0.0176(3) 0.9533(1)
O Ui/Ue*100	0.33(2)	0.66(4)
Bi-O lengths x 3 (Å)	2.5301(9)	2.504(1)
Bi-O lengths x3 (Å)	2.2765(13)	2.284(2)
Fe-O bond lengths x 3 (Å)	2.112(1)	2.108(2)
Fe-O bond lengths x 3 (Å)	1.950(1)	1.953(2)
Fe-O-Fe bond angle (°)	155.13	154.38(7)

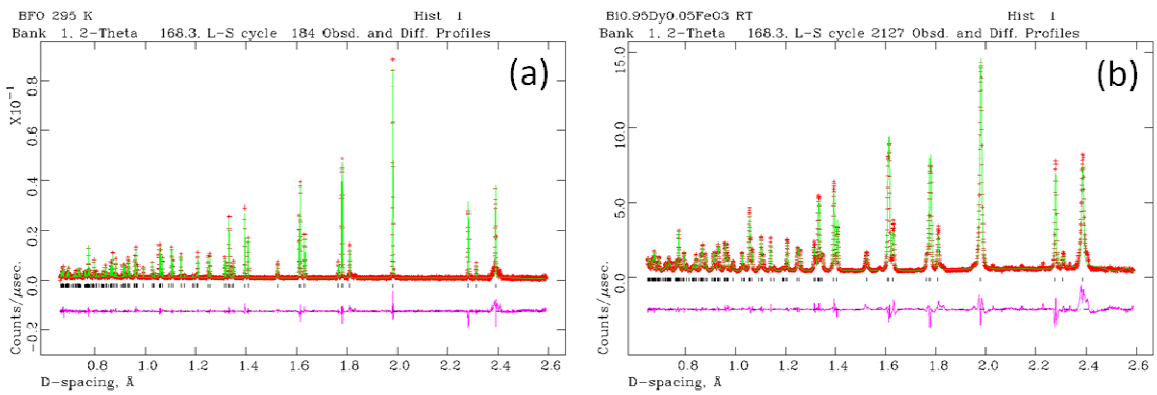

Figure S2: *Rietveld refinement profiles for data fitted using the R3c model to neutron diffraction data collected for (a) $BiFeO_3$ and (b) $Bi_{0.95}Dy_{0.05}FeO_3$. The red circles represent the observed data, the green line represents the calculated model and the pink line represents the difference.*

In order to try and model the peak broadening observed in the synchrotron diffraction data collected for $Bi_{0.95}Dy_{0.05}FeO_3$ refinements were performed using the *R*3*c* model for approximately 43 variables (including 18 background coefficient's fitted using a shifted Chebyschev function and 8 spherical Harmonic order (ODF) terms) with peak shape fitted using an expanded Pseudo-Voigt function to include Stephen's model for microstrain broadening.[3-7] This methodology allows for strain to effectively become described by the crystal symmetry and allows for anisotropic broadening. As with previous refinements of synchrotron diffraction data the U*iso* were fixed to 1.00 (Ui/Ue*100) and the fractional occupancies of the atoms not refined. Refinement parameters are given in table S3 with the refinement profiles in figure S3.

Table S3: *Rietveld refinement parameters for the refinement of powder synchrotron diffraction data collected for $Bi_{0.95}Dy_{0.05}FeO_3$ materials fitted using the rhombohedral, R3c model. Refinements with the peak shape fitted using a typical Pseudo-Voigt (type 2) and the expanded Pseudo-Voigt function (including Stephen's microstrain terms, type 4) are given for comparison.*

Parameter	**$Bi_{0.95}Dy_{0.05}FeO_3$ Type 2**	**$Bi_{0.95}Dy_{0.05}FeO_3$ Type 4**
R_{wp}	15.11	17.64
R_p	11.09	12.40
a (Å)	5.57447(5)	5.57487(4)
b (Å)	5.57447(5)	5.57487(4)
c (Å)	13.8541(2)	13.8547(2)
Cell Volume (Å)	372.835(7)	372.905(6)
Bi/Dy (0,0,0)		
Bi/Dy Ui/Ue*100	1.00	1.00
Fe (0,0,*z*)	0.2222(2)	0.2222(3)
Fe Ui/Ue*100	1.00	1.00
O (*x*,*y*,*z*)	0.446(3) 0.025(3) 0.955(1)	0.445(3) 0.025(3) 0.955(1)
O Ui/Ue*100	1.00	1.00
Texture Index	1.0070	1.0055
Bi-O lengths x 3 (Å)	2.50(1)	2.50(1)
Bi-O lengths x3 (Å)	2.28(1)	2.27(1)
Fe-O bond lengths x 3 (Å)	2.07(2)	2.08(2)
Fe-O bond lengths x 3 (Å)	1.99(2)	1.99(2)
Fe-O-Fe bond angle (°)	153.9(6)	153.7(7)

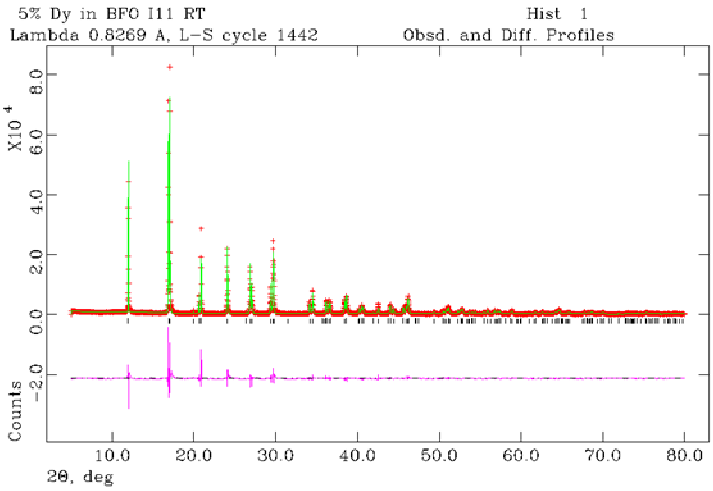

Figure S3: *Rietveld refinement profiles for synchrotron diffraction data collected for* $Bi_{0.95}Dy_{0.05}FeO_3$*data fitted using the R3c model and an expanded Pseudo-Voigt function to describe the peak shape. The red circles represent the observed data, the green line represents the calculated model and the pink line represents the difference.*

Lebail refinements were performed in order to investigate the validity of the *Cc* and *P*1 models to describe both the powder neutron and diffraction profiles observed for $Bi_{0.95}Dy_{0.05}FeO_3$. For comparison Lebail refinements were also performed using the *R*3*c* model. For synchrotron diffraction data refinements were performed for approximately 42 variables, including 18 background terms fitted using a shifted Chebyschev function. Peak shape was described using the expanded Pseudo-Voigt function. Powder neutron diffraction experiments were performed for 28 variables including 18 background coefficients fitted using a shifted Chebyschev function. Peak shape modelled using a Pseudo-Voigt function applicable for time-of-flight data and an absorption correction. Refinement data are given in the full manuscript. Refinement profiles for synchrotron and neutron diffraction data are given in figure S4.

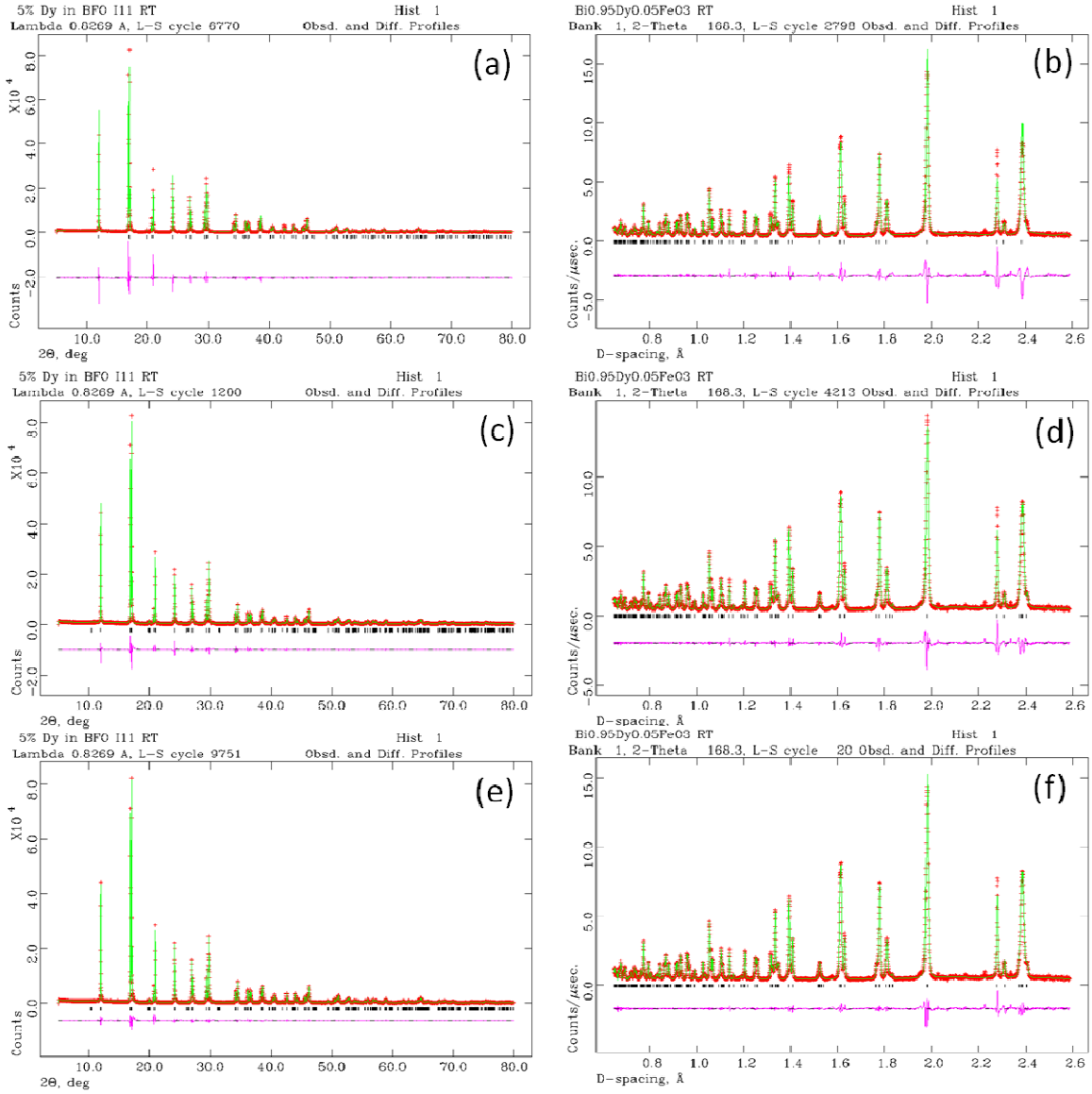

Figure S4: *Rietveld refinement profiles for synchrotron and neutron diffraction data collected for $Bi_{0.95}Dy_{0.05}FeO_3$ data fitted using the R3c ((a) and (b)), Cc ((c) and (d)) and P1 ((e) and (f)) models. The red circles represent the observed data, the green line represents the calculated model and the pink line represents the difference.*

The validity of the *Cc* model to describe both the powder neutron and diffraction profiles observed for $BiFeO_3$, $Bi_{0.98}Dy_{0.02}FeO_3$ and $Bi_{0.95}Dy_{0.05}FeO_3$ was further investigated by performing full Rietveld refinements. Synchrotron diffraction data refinements were performed for approximately 47 variables, including 18 background terms fitted using a shifted Chebyschev function, 8 spherical Harmonic order (ODF) terms to describe surface roughness. Since the peak shape in $BiFeO_3$ is sharp peak shape for all materials was described using the typical Pseudo-Voigt function. Attempts to further improve the observed

fits to the broadened peak observed in $Bi_{0.95}Dy_{0.05}FeO_3$ did not yield improved fits (not reported here). Powder neutron diffraction experiments were performed for 49 variables including 18 background coefficients fitted using a shifted Chebyschev function; peak shape modelled using a Pseudo-Voigt function applicable for time-of-flight data and an absorption correction. Refinement data are given in table S4 with refinement profiles given in figure S5.

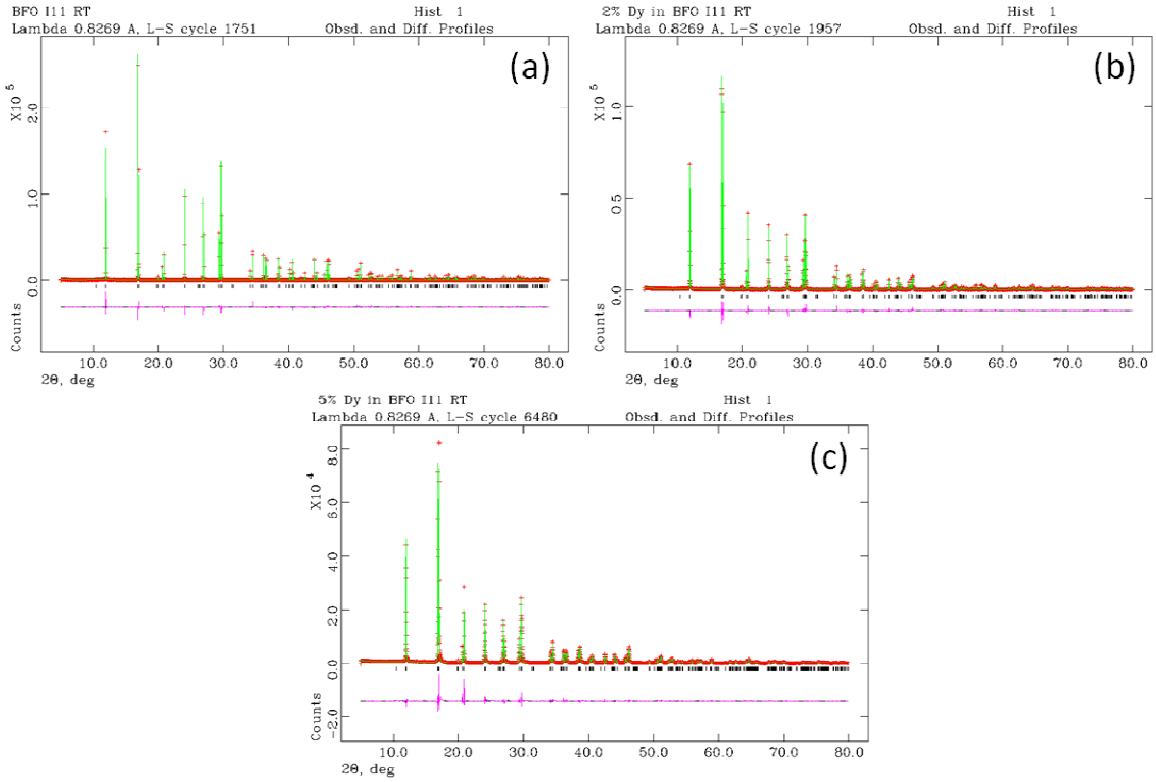

Figure S5: *Rietveld refinement profiles for synchrotron diffraction data collected for (a)* $BiFeO_3$*, (b)* $Bi_{0.98}Dy_{0.02}FeO_3$ *and (c) powder neutron diffraction data collected for* $BiFeO_3$ *fitted using the Cc model. The red circles represent the observed data, the green line represents the calculated model and the pink line represents the difference.*

Table S4: *Rietveld refinement parameters for the refinement of powder synchrotron and neutron diffraction data collected for $BiFeO_3$ and $Bi_{0.98}Dy_{0.02}FeO_3$ materials respectively using the monoclinic, Cc model. Full refinement parameters for $Bi_{0.95}Dy_{0.05}FeO_3$ refined using the Cc model are given in the full manuscript.*

Parameter	**Synchrotron**		**Neutron**
	$BiFeO_3$	**$Bi_{0.98}Dy_{0.02}FeO_3$**	**$BiFeO_3$**
R_{wp}	10.10	10.54	13.62
R_p	7.91	7.81	13.62
a (Å)	9.66381(5)	9.66204(7)	9.6695(1)
b (Å)	5.57867(3)	5.57721(4)	5.58156(6)
c (Å)	5.63436(3)	5.63159(4)	5.64024(6)
β (°)	124.8602(2)	124.8460(4)	124.8939(6)
Cell Volume (Å)	249.246(2)	249.055(3)	249.681(5)
Bi/Dy (0,¼,0)			
Bi/Dy Ui/Ue*100	1.00	1.00	0.30(3)
Fe (*x*,*y*,*z*)	0.2208(7) 0.250(2) 0.6640(4)	0.2213(8) 0.24740(1) 0.6665(5)	0.2212(4) 0.2605(4) 0.6633(2)
Fe Ui/Ue*100	1.00	1.00	0.03(3)
O1 (*x*,*y*,*z*)	-0.021(3) 0.188(5) 0.412(4)	-0.032(4) 0.200(6) 0.373(7)	-0.0390(7) 0.1801(8) 0.3602(9)
O1 Ui/Ue*100	1.00	1.00	0.05(8)
O2 (*x*,*y*,*z*)	0.158(3) 0.473(6) -0.142(6)	0.168(4) 0.484(9) -0.141(7)	0.1633(8) 0.489(1) -0.145(1)
O2 Ui/Ue*100	1.00	1.00	0.8(1)
O3 (*x*,*y*,*z*)	0.225(3) -0.034(5) -0.151(6)	0.240(4) -0.047(6) -0.173(5)	0.2274(8) -0.0334(9) -0.1437(9)
O3 Ui/Ue*100	1.00	1.00	0.3(1)
Texture Index	1.0217	1.0044	N/A
Bi-O lengths (Å)	2.47(3) 2.48(3) 2.43(3) 2.30(3) 2.27(3) 2.58(3)	2.31(4) 2.58(4) 2.54(4) 2.27(4) 2.28(3) 2.39(3)	2.302(5) 2.487(4) 2.533(7) 2.238(5) 2.298(5) 2.574(7)
Fe-O bond lengths (Å)	1.95(3) 2.08(3) 1.97(3) 2.13(3) 1.88(3) 2.17(3)	2.05(3) 1.99(4) 1.95(4) 2.12(4) 1.84(3) 2.31(3)	2.129(5) 1.942(5) 1.949(6) 2.045(5) 1.951(5) 2.174(5)
Fe-O-Fe bond angles (°)	160(2) 151(2) 156(2)	160(2) 156(2) 144(2)	154.0(3) 153.3(3) 154.9(4)

In order to investigate the amplitude of the Γ3 tilt on the atomic sites we looked more closely at our mode analysis. It is clear from figure S6 that the distortion mode has the largest effects on the O1 and O3 sites i.e. the equatorial oxygen sites resulting in a distortion of the octahedral and ultimately a change in the polarisation axis.

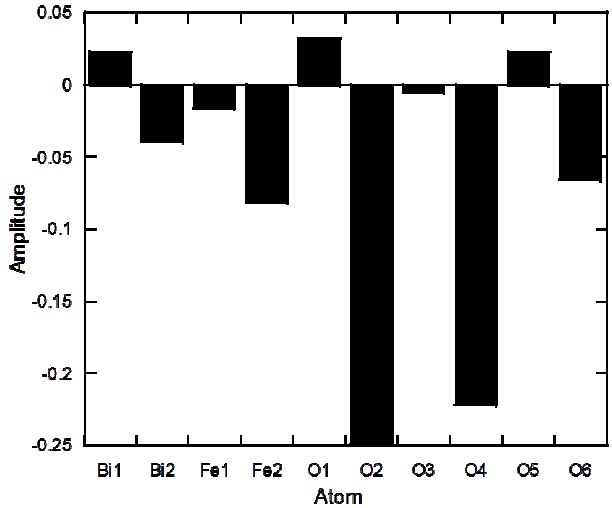

Figure S6: *Observed amplitudes of our symmetry mode analysis showing that the Γ3 mode has the most effect on the oxygen atoms labelled O2 and O4. In the ISODISTORT software these correlate with the oxygen sites in the* equatorial positions.

In order to investigate the lattice parameters and strain broadening in materials with $0.07 \leq x \leq 0.18$ were refined. Lebail refinements were performed due to correlation effects from multiple lattice parameters, and phases which exhibit very different peak shapes etc with refinements carried out as described above. Refinement parameters are given in tables S5 and S6 with the refinement profiles given in figure S7 and S8, and S9 for the refinements performed on synchrotron x-ray and neutron diffraction data respectively. No coherent trend is observed in the lattice parameters (not shown) for either phase this is most likely due to the increasing complexity of the data such that multiple phases showing slight variations in lattice parameters are observed. This is most evident in materials with dysprosium contents greater than x = 0.18 where the diffraction patterns clearly show a tailing of the peaks associated with the *Pnma* phase. These patterns are best modelled by two *Pnma* phase with differing lattice parameters. It should also be noted that the fits to the powder neutron diffraction data are further complicated by the quality of the data collected (as a result of absorption effects arising from increasing dysprosium contents), the presence of two distinct

magnetic phases coupled to the *Cc* and *Pnma* phases respectively as well as diffuse scattering contributions discussed in the manuscript.

Table S5: *Lebail refinement details for the mixed phase refinements of the synchrotron diffraction data collected for $Bi_{1-x}Dy_xFeO_3$ ($0.07 \leq x \leq 0.18$) modelled using the monoclinic, Cc, and orthorhombic Pnma space groups. Note: Atomic co-ordinates, thermal contributions (U_{iso}) and fractional occupancies were not refined. Bi0.82Dy0.18FeO3 was modelled with a Cc and two Pnma phases with different lattice parameters.*

Parameter		**x in $Bi_{1-x}Dy_xFeO_3$**						
		0.07	**0.10**	**0.12**	**0.14**	**0.16**	**0.18**	
Cc	R_{wp}	7.23	4.69	5.59	7.97	7.43	6.88	
	R_p	5.39	3.43	3.99	5.59	5.41	4.97	
	a (Å)	9.6561(1)	9.6466(2)	9.6472(2)	9.6576(2)	9.6394(2)	9.6478(2)	
	b (Å)	5.57113(8)	5.56777(6)	5.56738(8)	5.5682(1)	5.57268(7)	5.57554(6)	
	c (Å)	5.62382(7)	5.61395(7)	5.61397(8)	5.62097(9)	5.6119(1)	5.6151(1)	
	β (°)	124.8208(7)	124.7980(8)	124.8021(9)	124.8403(9)	124.7121(9)	124.734(1)	
	Cell Vol (Å^3)	248.364(6)	247.603(6)	247.589(7)	248.090(8)	247.801(8)	248.222(7)	
	LY	17.35(2)	24.81(2)	25.25(2)	15.44(3)	13.87(3)	19.19(3)	
Pnma	**a (Å)**	5.6222(2)	5.6288(2)	5.6288(3)	5.6300(1)	5.6272(2)	5.6292(1)	5.607(1)
	b (Å)	7.8031(4)	7.8084 (3)	7.8053(5)	7.7980(3)	7.8007(3)	7.8014(2)	7.7815(9)
	c (Å)	5.4372(5)	5.4183(3)	5.4193(4)	5.4214(2)	5.4236(2)	5.4229(2)	5.317(1)
	Cell Vol (Å^3)	238.53(3)	238.14(2)	238.10(2)	238.01(1)	238.08(1)	238.15(1)	231.96(8)

Table S6: *Lebail refinement details for the mixed phase refinements of the neutron diffraction data collected for $Bi_{1-x}Dy_xFeO_3$ ($0.07 \leq x \leq 0.25$) modelled using the monoclinic, Cc, and orthorhombic Pnma space groups. Note: Atomic co-ordinates, thermal contributions (U_{iso}) and fractional occupancies were not refined.*

Parameter		x in $Bi_{1-x}Dy_xFeO_3$					
		0.07	**0.10**	**0.12**	**0.16**	**0.18**	**0.25**
Cc	R_{wp}	4.68	3.69	4.83	5.33	5.95	4.21
	R_p	4.78	3.68	5.20	5.57	5.65	4.33
	a (Å)	9.6507(2)	9.6410(2)	9.6472(2)	9.6530(3)	9.6366(4)	9.6408(9)
	b (Å)	5.5751(3)	5.5724(2)	5.5767(2)	5.5742(4)	5.5879(2)	5.5784(4)
	c (Å)	5.6264(1)	5.62233(8)	5.6277(1)	5.6280(2)	5.6296(2)	5.6276(4)
	β (°)	124.8810(8)	124.914(2)	124.919(2)	124.886(3)	124.775(3)	124.782(5)
	Cell Vol ($Å^3$)	248.34(1)	247.69(1)	248.26(1)	248.40(2)	249.00(2)	248.58(4)
Pnma1	**a (Å)**	5.6316(3)	5.6246(2)	5.6242(3)	5.6215(3)	5.6314(2)	5.6321(1)
	b (Å)	7.8201(8)	7.8032(7)	7.8041(5)	7.8189(6)	7.7937(4)	7.7701(2)
	c (Å)	5.4113(3)	5.4233(3)	5.4242(4)	5.4269(4)	5.4149(3)	5.4045(1)
	Cell Vol ($Å^3$)	238.31(3)	238.03(3)	238.08(3)	238.54(3)	237.65(2)	236.512(9)
Pnma2	**a (Å)**					5.703(3)	5.5909(9)
	b (Å)					7.744(2)	7.7172(6)
	c (Å)					5.409(2)	5.383(1)
	Cell Vol ($Å^3$)					238.8(2)	232.24(6)

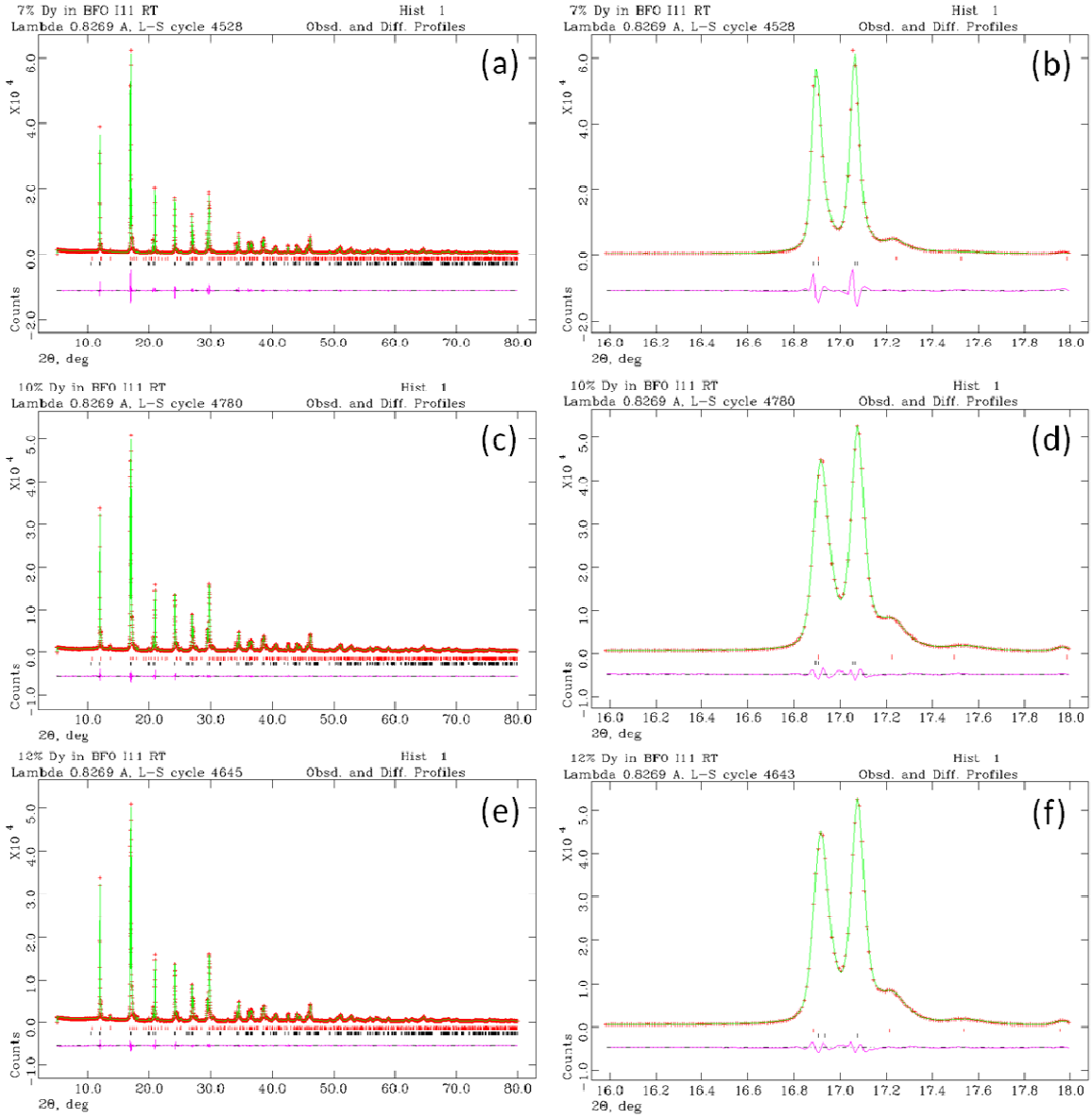

Figure S7: *Lebail refinement profiles for synchrotron diffraction data collected for* $Bi_{0.93}Dy_{0.07}FeO_3$ *((a) and (b)),* $Bi_{0.90}Dy_{0.10}FeO_3$ *((c) and (d)),* $Bi_{0.88}Dy_{0.12}FeO_3$ *((e) and (f)) fitted using contributions from both the Cc and Pnma models. The red circles represent the observed data, the green line represents the calculated model and the pink line represents the difference.*

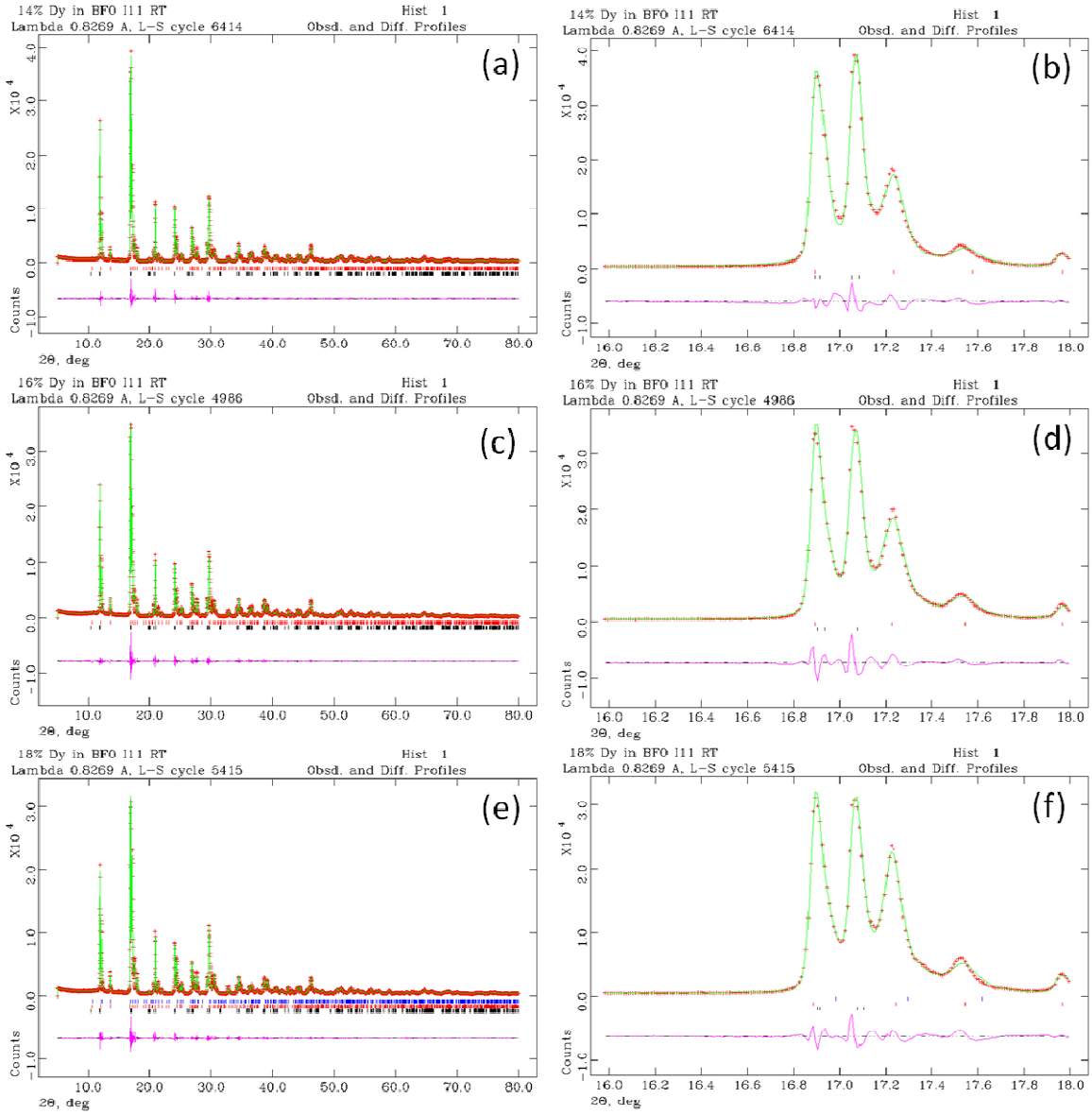

Figure S8: *Lebail refinement profiles for synchrotron diffraction data collected for* $Bi_{0.86}Dy_{0.14}FeO_3$ *((a) and (b)),* $Bi_{0.84}Dy_{0.16}FeO_3$ *((c) and (d)),* $Bi_{0.82}Dy_{0.18}FeO_3$ *((e) and (f)) fitted using contributions from both the Cc and Pnma models. The red circles represent the observed data, the green line represents the calculated model and the pink line represents the difference. Note* $Bi_{0.82}Dy_{0.18}FeO_3$ *was best modelled with a mixture of Cc and two Pnma phases.*

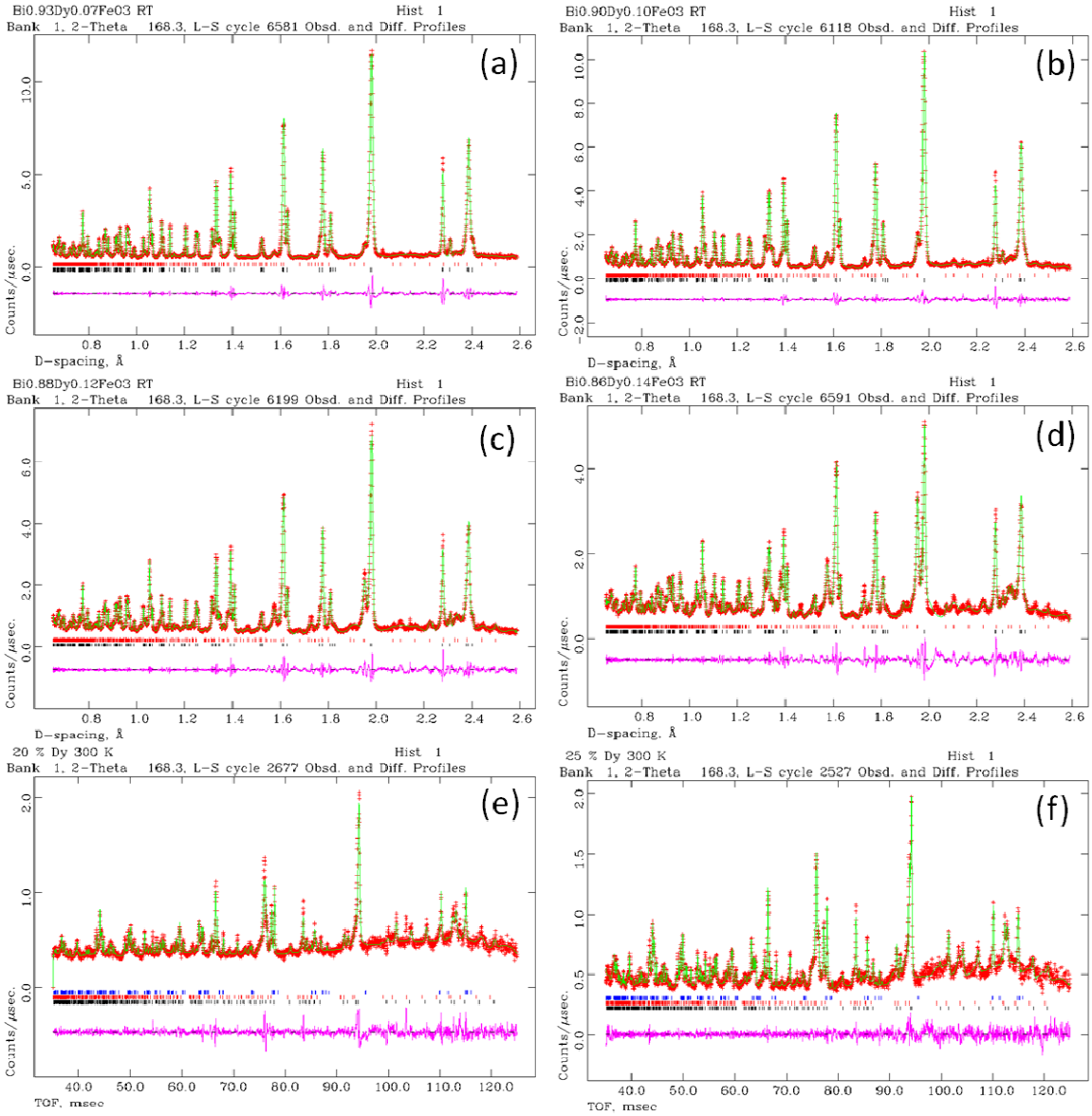

Figure S9: *Lebail refinement profiles for neutron diffraction data collected for (a)* $Bi_{0.93}Dy_{0.07}FeO_3$*, (b)* $Bi_{0.90}Dy_{0.10}FeO_3$*, (c)* $Bi_{0.88}Dy_{0.12}FeO_3$*, (d)* $Bi_{0.84}Dy_{0.16}FeO_3$*, (b)* $Bi_{0.82}Dy_{0.18}FeO_3$ *and (c)* $Bi_{0.75}Dy_{0.25}FeO_3$ *fitted using contributions from both the Cc and Pnma models. The red circles represent the observed data, the green line represents the calculated model and the pink line represents the difference. Note* $Bi_{0.82}Dy_{0.18}FeO_3$ *was best modelled with a mixture of Cc and two Pnma phases.*

Refinement parameters for the Rietveld refinement of $Bi_{0.70}Dy_{0.30}FeO_3$ are given in table S7. Refinements were performed for 52 and 71 variables for powder neutron and synchrotron diffraction data respectively. In both cases the background was described by 18 shifted Chebyschev terms with peak shape fitted using a Pseudo-Voigt function. In addition 8 spherical Harmonic order (ODF) terms to describe surface roughness and absorption coefficient to describe absorption effects were refined in synchrotron x-ray and neutron diffraction data respectively. Refinements were difficult to perform due to multiple parameters arising from multiple phases. We note that negative thermal parameters are observed in the second *Pnma* phase refined in the neutron data. Whilst we recognise these as nonsensical we believe that this does not suggest limitations of the phase model but rather limitations of the data.

Table S7: *Rietveld refinement details for the mixed phase refinements of the neutron and synchrotron x-ray diffraction data collected for* $Bi_{0.70}Dy_{0.30}FeO_3$ *modelled using two orthorhombic Pnma models with different lattice parameters. Note: Atomic co-ordinates, thermal contributions* (U_{iso}) *and fractional occupancies were not refined.*

Parameter	**Synchrotron**		**Neutron**	
	Pnma 1	**Pnma 2**	**Pnma 1**	**Pnma 2**
R_{wp}	7.45		2.80	
R_p	5.62		2.93	
a (Å)	5.6210(3)	5.63176(5)	5.6266(3)	5.615(1)
b (Å)	7.7474(7)	7.7842(1)	7.7862(4)	7.723(2)
c (Å)	5.3921(6)	5.41591(8)	5.4187(3)	5.383(1)
Cell Volume (Å^3)	234.82(3)	237.425(5)	237.39(2)	233.4(1)
Bi/Dy (*x*,¼,*z*)	0.0512(3) -0.0040(8)	0.031(1) 0.033(1)	0.0511(4) -0.0119(7)	0.061(1) -0.010(3)
Bi/Dy Ui/Ue*100	1.00	1.00	1.06(10)	1.2(3)
Fe (0,0,½)				
Fe Ui/Ue*100	1.00	1.00	0.3(1)	-1.3(2)
O1 (*x*,¼,*z*)	0.422(7) 0.125(5)	0.482(2) 0.079(3)	0.4757(9) 0.1016(9)	0.468(3) 0.112(2)
O1Ui/Ue*100	1.00	1.00	0.8(1)	-2.4(3)
O2 (*x*,*y*,*z*)	-0.313(4) -0.043(3) 0.336(5)	-0.293(2) -0.063(2) 0.298(2)	-0.2977(7) -0.0432(5) 0.3024(8)	-0.294(3) -0.051(3) 0.308(3)
O3 Ui/Ue*100	1.00	1.00	1.7(1)	-0.8(3)
Bi-O lengths (Å)	2.20(4) 2.17(3) 2.26(2) 2.26(2) 2.82(2) 2.56(2) 2.82(2) 2.56(2)	2.55(1) 2.12(2) 2.35(1) 2.35(1) 2.74(1) 2.78(1) 2.74(1) 2.78(1)	2.467(6) 2.263(6) 2.375(4) 2.375(4) 2.645(5) 2.688(4) 2.645(5) 2.688(4)	2.37(2) 2.21(2) 2.36(2) 2.36(2) 2.58(2) 2.69(2) 2.58(2) 2.69(2)
Fe-O bond lengths (Å)	2.10(1) 2.10(1) 2.00(3) 2.12(3) 2.00(3) 2.12(3)	1.996(3) 1.996(3) 2.04(1) 2.05(1) 2.04(1) 2.05(1)	2.028(1) 2.028(1) 2.016(4) 2.023(4) 2.016(4) 2.023(4)	2.029(4) 2.029(4) 1.99(1) 2.06(1) 1.99(1) 2.06(1)
Fe-O-Fe bond angles (°)	135(2) 142(1)	154.4(8) 145.6(6)	147.5(3) 150.4(2)	144.3(7) 147.9(8)

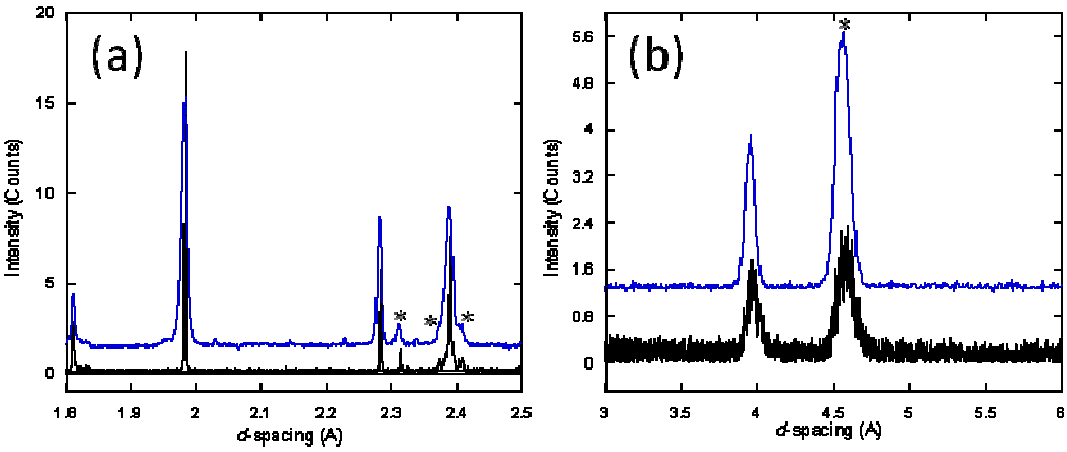

Figure S10: *Comparison of the powder neutron diffraction data collected for $BiFeO_3$ (black line) and $Bi_{0.95}Dy_{0.05}FeO_3$ (blue line) showing the similarities in magnetic Bragg peaks in (a) HRPD bank 1 and (b) HRPD bank 3 suggesting that both material exhibit a complex magnetic spin cycloid spin arrangement. Note the $BiFeO_3$ pattern has been scaled and the $Bi_{0.95}Dy_{0.05}FeO_3$ has been offset for comparison.*

References

[1] A. C. Larson, R. B. V. Dreele, *Los Alamos National Laboratory Report LAUR* **96**, *86*.

[2] B. H. Toby, *J. Appl. Cryst.* **2001**, *34*, 210.

[3] B. van Laar, W. B. Yelon, *J. Appl. Cryst.* **1984**, *17*, 47.

[4] C. J. Howard, *J. Appl. Cryst.* **1982**, *15*, 615.

[5] L. W. Finger, D. E. Cox, A. P. Jephcoat, *J. Appl. Cryst.* **1994**, *27*, 892.

[6] P. Thompson, D. E. Cox, J. B. Hastings, *J. Appl. Cryst.* **1987**, *20*, 79.

[7] P. Stephens, *J. Appl. Cryst.* **1999**, *32*, 281.